51st AIAA Aerospace Sciences Meeting including the New Horizons Forum and Aerospace Exposition
07 - 10 January 2013, Grapevine (Dallas/Ft. Worth Region), Texas
AIAA 2013-0172

Large Eddy Simulation of a Gas Turbine Model Combustor

Yee Chee See* and Matthias Ihme†
Department of Aerospace Engineering, University of Michigan
Ann Arbor, MI 48109

I. Introduction

The current design of gas-turbine (GT) systems is driven by the need for increased power-densities, improved fuel-efficiencies, and reduced life cycle costs and environmental impact. Computational techniques have the potential for providing valuable information for the design of GT combustion systems, if adequate models are available. Over recent years, remarkable progress has been made in the development of high-fidelity combustion models and numerical techniques for turbulent reacting flows. In particular, the LES technique has been demonstrated to provide considerably improved predictions for scalar mixing processes compared to Reynolds-averaged Navier-Stokes (RANS) approaches. This improved predictive capability is attributed to the fact that in LES the energy-containing and large-scale coherent structures are fully resolved, and only effects of numerically unresolved turbulent scales require modeling. These small scales, however, are more homogeneous so that more universal closure models can be utilized. Over recent years, different LES combustion models have been developed, including level-set formulations,[1–7] conditional moment closure models,[8–12] thickened flamelet models,[13–15] transported PDF methods,[16–18] and flamelet-based combustion models.[19–24] However, these models have been largely developed and validated in the context of canonical and geometrically unconfined flame-configurations, such as jet-flames or simple dump-combustors. Furthermore, LES-calculations in complex burner-configuration that are relevant to realistic gas-turbine combustor and operating conditions have so far not been fully utilized. This shortcoming can be attributed to the following reasons: (i) Absence of high-fidelity computational models that can accurately describe the turbulent combustion processes and coupling between turbulence, reaction chemistry, and scalar mixing; (ii) Lack of experimental data to enable comprehensive model-validation; (iii) Geometric complexity and construction of geometry-conform meshes for complex combustor geometries; (iv) Highly transient combustion regime, topologic asymmetry, and flow-field sensitivity and solution-dependence on grid-resolution and numerical accuracy; and (v) Computational complexity and necessary requirements for accurately resolving relevant spatio-temporal scales.

Apart from very few exceptions, LES-calculations of gas-turbine combustors have so far been performed under drastically simplified conditions, limited or no comparison with experimental data, and by employing significant simplifications in the description of the combustion model (*i.e.,* utilizing one-step reaction chemistry, ambient operating conditions, and restriction to gaseous fuel combustion).

*Research Assistant, Department of Aerospace Engineering, University of Michigan, AIAA member
†Assistant Professor, Department of Aerospace Engineering, University of Michigan,AIAA member

The objective of this work is to conduct large-eddy simulations (LES) of a gas-turbine model combustor (GTMC) at relevant operating conditions in order to assess the accuracy and capability of current LES-combustion and subgrid-scale models. In this investigation, simulations of isothermal and reacting operating conditions are considered, and modeling results are compared against experimental data. After summarizing the LES-methodology in the next section, the experimental configuration is presented in Sec. III. Modeling results for the isothermal and reacting operating conditions are presented in Sec. IV, and the paper finishes with conclusions.

II. Methodology

A. Governing Equations

In LES, the coherent large scale turbulent structures are computationally resolved while the effect on the smaller structures are modeled. To achieve this in an reacting flow, the flow quantities are low-pass filtered in the framework of Favre-averaging. The Favre-filtered quantity of a scalar Ψ is computed as:

$$\widetilde{\Psi}\left(t,\boldsymbol{x}\right)=\frac{1}{\rho}\int\rho\left(t,\boldsymbol{x}\right)\Psi\left(t,\boldsymbol{x}\right)\mathcal{G}\left(t,\boldsymbol{x},\boldsymbol{y};\Delta\right)d\boldsymbol{y}\ , \tag{1}$$

where Δ is the LES filter width and $\mathcal{G}$ is the low-pass filter. After multiplying the conservation equations by $\mathcal{G}$ and integrating over the domain, the following Favre-filter equations are obtained:

$$\widetilde{D_t}\bar{\rho}=-\bar{\rho}\nabla\cdot\widetilde{\mathbf{u}}, \tag{2a}$$

$$\bar{\rho}\widetilde{D_t}\widetilde{\mathbf{u}}=-\nabla\bar{p}+\nabla\cdot\underline{\underline{\widetilde{\tau}}}-\nabla\cdot\underline{\underline{\tau}}^{res}, \tag{2b}$$

$$\bar{\rho}\widetilde{D_t}\widetilde{Z}=\nabla\cdot\left(\bar{\rho}\widetilde{\alpha}\nabla\widetilde{Z}\right)-\nabla\cdot\tau_Z^{res}, \tag{2c}$$

$$\bar{\rho}\widetilde{D_t}\widetilde{C}=\nabla\cdot\left(\bar{\rho}\widetilde{\alpha}\nabla\widetilde{C}\right)-\nabla\cdot\tau_C^{res}+\overline{\dot{\Omega}}_C, \tag{2d}$$

$$\bar{\rho}\widetilde{D_t}\widetilde{Q}=\nabla\cdot\left(\bar{\rho}\widetilde{\alpha}\nabla\widetilde{Q}\right)-\nabla\cdot\tau_Q^{res}+\overline{\dot{\Omega}}_Q, \tag{2e}$$

where $\mathbf{u}$ is the velocity vector, ρ is the density, p is the pressure, Z is the mixture fraction, $Q=Z^2$ is the second moment of Z, C is the reaction progress variable, D_t is the substantial derivative, $\underline{\underline{\tau}}$ is the viscous shear stress tensor, α is species diffusivity, $\overline{\dot{\Omega}}_C$ and $\overline{\dot{\Omega}}_Q$ are the source terms for $\widetilde{C}$ and $\widetilde{Q}$, respectively, and the superscript "res" refers to the residual stresses.

The low Mach-number LES solver VIDA was employed to numerically solve Eq. (2). For the spatial discretization, the solver uses a scheme developed by Ham et al.[25,26] which is formally second order accurate on unstructured meshes. Time-advancement is achieved through a second-order accurate predictor-corrector scheme, which is detailed in the work by Ham.[27] Due to the low-Mach-number assumption, the pressure is described as solution to a Poisson equation, which is solved using a parallel multi-grid solver.[28]

B. Subgrid Scale Model

The residual stresses and turbulent scalar fluxes appearing in the Favre-filtered equations, (2), require modeling. In the following the residual stress tensor $\underline{\underline{\tau}}^{res}$ is evaluated using the eddy-viscosity model, *i.e.,*

$$\underline{\underline{\tau}}^{res}=\bar{\rho}\widetilde{\mathbf{u}}\widetilde{\mathbf{u}}-\bar{\rho}\widetilde{\mathbf{u}\mathbf{u}}=2\bar{\rho}\nu_t\underline{\underline{\widetilde{S}}}\ , \tag{3}$$

where $\underline{\underline{\widetilde{S}}}$ is the strain rate and ν_t is the turbulent viscosity. The residual scalar flux is computed as

$$\tau_\Psi^{res}=\bar{\rho}\widetilde{\mathbf{u}}\widetilde{\Psi}-\bar{\rho}\widetilde{\mathbf{u}\Psi}=\bar{\rho}\alpha_t\nabla\widetilde{\Psi}\ . \tag{4}$$

The production term for $\widetilde{Q}$ is expressed in terms of the mixture fraction variance and the scalar dissipation rate:

$$\dot{\Omega}_Q = -C_Q \bar{\rho} \alpha_t \frac{\widetilde{Z''^2}}{\Delta^2} - 2\bar{\rho}\alpha |\nabla \widetilde{Z}|^2 \,, \tag{5}$$

where C_Q is the mixing time-scale parameter.

In the present study, we consider the dynamic Smagorinsky model (DSM) and the Vreman model for the representation of the residual turbulent stresses. In the DSM-formulation the turbulent viscosity and diffusivity are related to the filtered shear-stress:

$$\nu_t = C_\nu \Delta^2 |\widetilde{\underline{\underline{S}}}|, \tag{6}$$

$$\alpha_\Psi = C_\Psi \Delta^2 |\widetilde{\underline{\underline{S}}}| \,, \tag{7}$$

and the coefficients C_ν and C_Ψ are evaluated using the dynamic version of Germano's procedure with Lilly's modification.[29,30] However, the application of this dynamic procedure can yield negative coefficients which can destabilize a numerical simulation. This problem can be circumvented by averaging over homogeneous directions. Due to the lack of axis-symmetry in some sections of the GTMC, the following simulations can only employ simple spatial averaging over the neighboring cells. To overcome this issue we also consider Vreman's model.[31] In this model the eddy viscosity is computed as:

$$\nu_t = C_s \left(\frac{\beta_{11}\beta_{22} - \beta_{12}^2 + \beta_{11}\beta_{33} - \beta_{13}^2 + \beta_{22}\beta_{33} - \beta_{23}^2}{\frac{\partial \widetilde{u}_k}{\partial x_l}\frac{\partial \widetilde{u}_k}{\partial x_l}} \right)^{1/2} . \tag{8}$$

where the tensor β_{ij} is determined as:

$$\beta_{ij} = \Delta^2 \frac{\partial \widetilde{u}_k}{\partial x_i}\frac{\partial \widetilde{u}_k}{\partial x_j} \,. \tag{9}$$

Unlike DSM, the coefficient C_s is a constant and is set to 0.1. This model was shown to recover vanishing eddy-viscosity near walls. In this model, the eddy diffusivity is then related to ν_t using a turbulent Schmidt number:

$$\alpha_t = \frac{\nu_t}{\mathrm{Sc}_t} \,. \tag{10}$$

C. Combustion Model

A flamelet/progress variable (FPV) model[20,32] is employed to close the Favre-filtered conservation equations and to express all thermochemical quantities in terms of mixture fraction and reaction progress variable. The FPV approach is based on the laminar flamelet assumption, in which a turbulent diffusion flame is considered as an ensemble of laminar flamelets.[33,34] In the flamelet regime, chemical reactions and heat transfer occur in a sufficiently thin layer that is deformed and stretched by the surrounding turbulence. To utilize the flamelet model in LES, the ensemble of flamelets are first precomputed by solving the steady one-dimensional laminar flamelet equations. Following the FPV formulation, the flamelet solution is parameterized in terms of mixture fraction and a progress variable:

$$\phi = \phi(Z, C), \tag{11}$$

where $\phi = (T, \mathbf{Y}, \dot{\Omega}_C, \rho, \mu, \alpha)^T$. This parameterization is expressed in terms of Favre-averaged quantities by employing a presumed probability density function (PDF) closure. To this end, Eq. (11) is integrated over a joint presumed PDF for mixture fraction and progress variable:

$$\widetilde{\phi} = \iint \phi(Z, C) \widetilde{P}(Z, C) dZ dC, \tag{12}$$

and $\widetilde{P}(Z,C)$ is modeled as:

$$\widetilde{P}(Z,C) = \beta(Z;\widetilde{Z},\widetilde{Z''^2})\delta(\widetilde{C}-C|Z)\ , \tag{13}$$

where β is the beta-distribution and δ is the Dirac delta function.

III. Experiment Configuration and Computational Setup

A. Experimental Configuration

In this work, we considered the gas turbine model combustor (GTMC) that was experimentally investigated by Weigand et al.[35,36] A schematic of the burner is illustrated in Fig. 1. The injector consists of a central air nozzle, an annular fuel nozzle, and a co-annular outer air nozzle. Both air nozzles supply swirling air at ambient temperature from a common plenum. The inner air nozzle has a diameter of 15 mm; the annular nozzle has an inner diameter of 17 mm and an outer diameter of 25 mm. Non-swirling fuel is provided through three exterior ports. The exit plane of the central air nozzle and fuel nozzle lies 4.5 mm below the exit plane of the outer air annulus, resulting in the formation of a partially-premixed and lifted flame base. The combustion chamber has a square cross section of 85 mm in width and 110 mm in height. The exit of the combustion chamber is an exhaust tube with a diameter of 40 mm and a height of 50 mm.

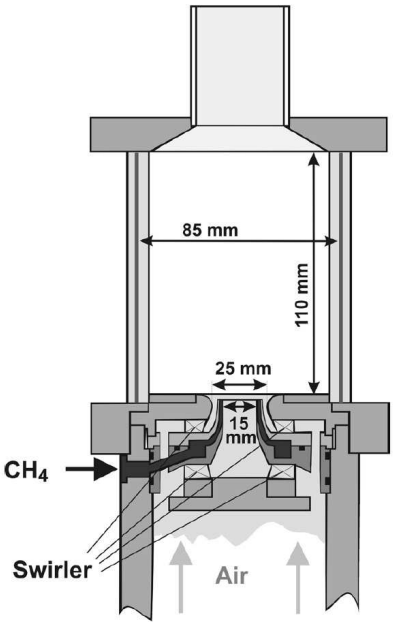

Figure 1. Schematic of gas turbine model combustor.[35,36]

The operating point that is investigated in this numerical study is "Flame A" which is classified by a thermal power, P_{th}, of 34.9 kW and a global equivalence ratio of $\Phi_{glob} = 0.65$. The corresponding mass flow rate for air and fuel are 1095 g/min and 41.8 g/min, respectively. In addition, the inlet temperature T_{in} was maintained at 295 K and the Reynolds number based on the minimum outer nozzle diameter is 58,000. At these inlet conditions, Weigand et al.[35] reported that the flame is acoustically stable but is lifted from the fuel nozzle exit. Although the flame is stable, the flow is highly unsteady because of the vortex breakdown that leads to an inner recirculation zone (IRZ). Due to the confined geometry of the burner, the outer recirculation zone (ORZ) is also present in the combustion chamber. Besides the reacting case, this study also considers a non-reacting case to investigate the isothermal flow-field structure in absence of heat and chemical reaction. These non-reacting experiments were conducted at conditions similar to that of Flame A, with reported mass flow-rates of 1184 g/min and 75.4 g/min through the outer and inner swirler.[37]

B. Computational Grid and Parameters

The GTMC was discretized using an unstructured mesh of 8.3 millions elements. The mesh is illustrated in Fig. 2, and consists of three sections for plenum, nozzle, and combustion chamber. The distribution of elements between the three meshes is summarized in Tab. 1. Widenhorn et al.[37] have noted that the flow inside the combustion chamber exhibits a pronounced sensitivity to the flow separation at the expansion section of the nozzle. Therefore, special care has been taken during the grid generation to ensure that the wall in this section is adequately resolved. For the mesh shown in Fig. 2 the mesh resolves the viscous sublayer with $\Delta y^+ \leq 1$, so that no wall function was employed.

Mesh Section	Number of Elements	Elements Type
Plenum	0.4 million	Hexahedral-dominant
Swirler	1.1 million	Pure Tetrahedral
Combustion Chamber	5.3 million	Hexahedral-dominant

Table 1. Description of the computational mesh.

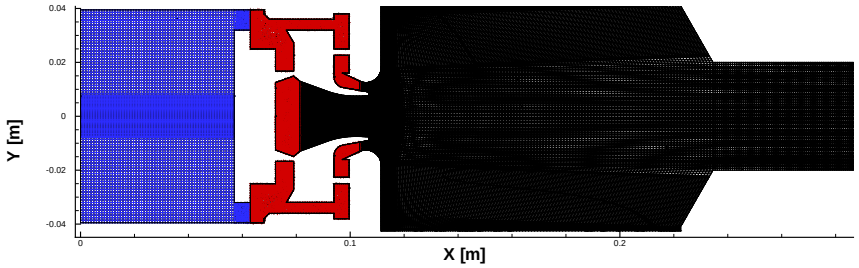

Figure 2. Computational mesh, showing a cross-section of the unstructured mesh with the plenum mesh in blue, the swirler-mesh in red, and the combustion-chamber mesh in black.

Boundary conditions at the plenum inlet and at the fuel injector are specified in accordance with the experimentally reported data. No turbulence was imposed at the inlet and a constant inflow profile was prescribed. At the combustor exit, convective outflow boundary conditions were used.

The reaction chemistry was described using the GRI 2.11 chemical mechanism, containing 227 elementary chemical reactions among 49 species. The progress variable employed in the following reacting LES was defined as[38] $Y_{CO_2} + Y_{CO} + Y_{H_2O} + Y_{H_2}$.

IV. Results and Discussion

A. Non-Reacting Simulation Results

LES computations of the non-reacting case using the DSM and Vreman model were performed. The simulations were initiated with a flow at rest, and initialization was conducted over two flow-through-times until the flow reached a statistical stationary state. The characteristic flow-through time was based on the combustor residence time, and corresponds to 30 ms. Following this initialization phase, statistical results were collected over a duration of approximately one flow-through-time.

Statistical results obtained from this simulation at different heights h above the combustor exit plane are presented in Figs. 3 and 4. Symbols denote experimental results, and simulation results using DSM and Vreman model are shown, respectively, by blue and red lines. Overall, the simulation results using the Vreman-model are in reasonable agreement with the experimental measurements, and agreement between simulation and measurements improves with increasing downstream distance. Comparison of results for the cross-stream velocity components $\widetilde{v}$ and $\widetilde{w}$ show that the simulation overpredicts the peak-values at $h = 2.5$ and 5 mm. Although the mean axial velocity component shows slightly sharper peaks, the simulation under-predict the vortex core near the nozzle exit. This suggests that the simulation predicts an elongated internal recirculation zone near the burner face. This recirculation zone extends in upstream direction, which can be seen from the strong reverse-flow in Fig. 3.

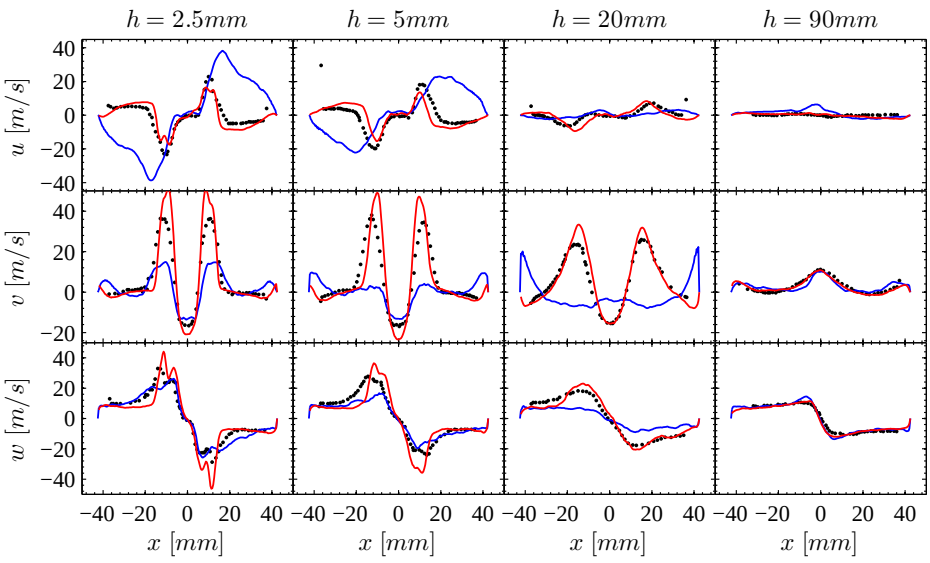

Figure 3. Comparison of mean velocity between experimental measurement (symbols), LES with DSM model (blue line) and LES with Vreman model (red line) for non-reacting configuration.

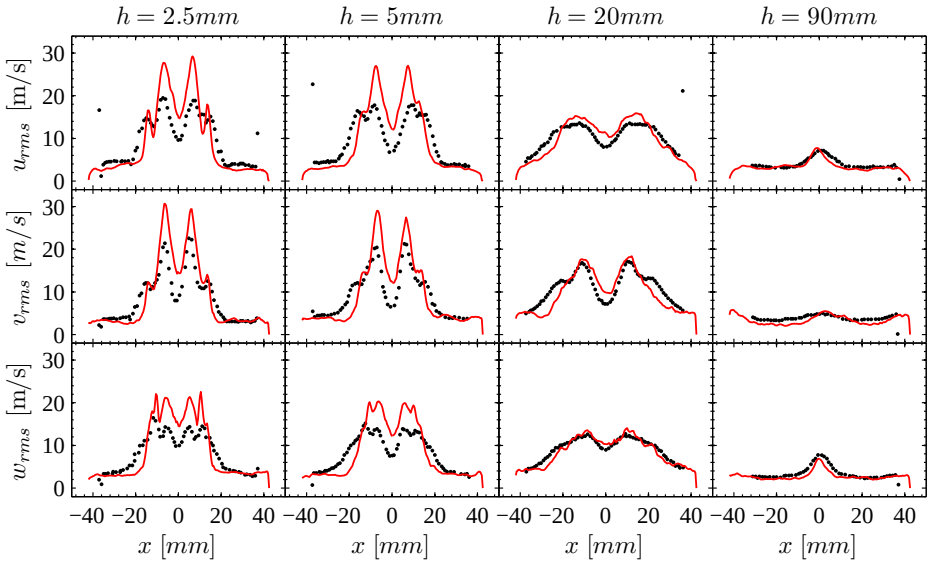

Figure 4. Comparison of rms velocity between experimental measurement (symbols), LES with DSM model (blue line) and LES with Vreman model (red line) for non-reacting configuration.

Given the complexity of this combustor configuration, good agreement for the root-mean-square (rms) velocity components is obtained with the Vreman SGS-model and the peak-locations for $h = 2.5$ and 5 mm are reasonably well predicted. The pronounced and highly localized velocity fluctuations appear to result from a shear-layer that is formed between the precessing vortex core and the outer recirculation region. The overprediction of the turbulence fluctuations may be attributed to an underprediction of the turbulent viscosity by the LES subgrid scale model in the near-field of the nozzle exit. Higher viscosity is known to dampen flow-field fluctuations and is also responsible for the broadening of the shear-layer. Therefore, a lower turbulent viscosity may lead

to stronger fluctuations and steeper shear-layers, which is observed from the simulations. However, other factors such as boundary conditions and mesh-resolution can also affect the predicted flow-field structure at the nozzle-exit.

The reconcile the hypothesis for the low turbulent viscosity, a simulation using the DSM-subgrid closure was performed. Starting from identical initial conditions, this computation was conducted over three flow-through-times to obtain a statistically-stationary flow. A qualitative examination of the instantaneous flow-field results with the previous simulation revealed visible disagreement. To quantify these discrepancies, the simulation was continued long enough to collect sufficiently converged mean-velocity statistics. The mean velocity components of this simulation are shown in Fig. 3 by blue lines. Clearly, the LES result obtained using DSM does not agree with the experiment. The predicted mean axial velocity at locations $h = 2.5$ mm and $h = 5$ mm is considerably larger than predicted with the Vreman model or observed experimentally. Moreover, the mean cross-stream velocity-components are significantly shifted away from the combustor core at $h \leq 20$ mm. These flow features are indicative for the presence of an extended inner recirculation zone in the combustor.

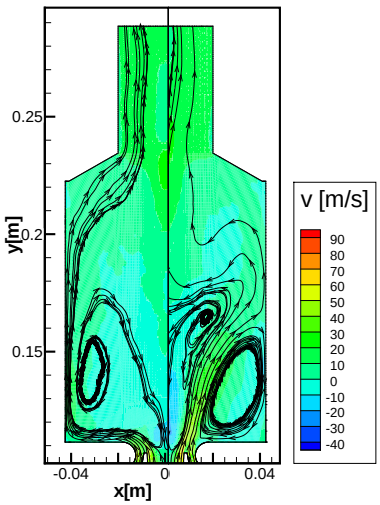

Figure 5. Comparison of streamlines in combustion chamber for LES with DSM model (left) and Vreman model (right).

To compare the predicted size of the inner recirculation zone obtained from both simulation, we present an instantaneous velocity field and streamlines in Fig. 5. The figure on the left is obtained with the DSM-closure, and the Vreman model was used to obtain the simulation results that are shown on the right of this figure. The streamlines shown in the right figure capture the experimentally observed inner and outer recirculation zones. However, the DSM-based simulation produced streamlines that correspond to a bifurcated recirculation structure, in which the flow exiting from the outer swirler doesn't separate, resulting in the suppression of the outer recirculation region. The here reported sensitivity of the flow-field structure to the subgrid-model may be attributed to the numerical resolution of the outer separation region. Therefore, further mesh-refinement studies are necessary to address this issues.

B. Reacting Simulation Results

It was shown in the previous section that the Vreman subgrid-closure accurately captures the non-reacting flow-field structure. Therefore, the following reacting flow-field simulations are all performed using this submodel. The reacting simulation was initialized with the cold-flow simulation. After igniting the flame by setting the progress variable to the equilibrium value in a region near the nozzle-exit, the simulation was continued for approximately two flow-through times in order to flush out all transient states. Statistics are then collected over a duration of two flow-through times. Simulation results for mean-flow quantities of velocity, temperature, mixture fraction, and species mass fraction of CO_2 are presented in Figs. 6 and 7.

The velocity statistics, shown in Fig. 6, are in reasonable agreement with the experimental measurements. Although the discrepancies are smaller than observed for the non-reacting simulation, similar factors regarding grid-resolution and statistical convergence could partially be responsible for these differences. It can also be seen that the reactive case exhibits similar recirculation structures as seen in the non-reacting configuration.

Statistical results for temperature and species mass fractions are presented in Fig. 7. Com-

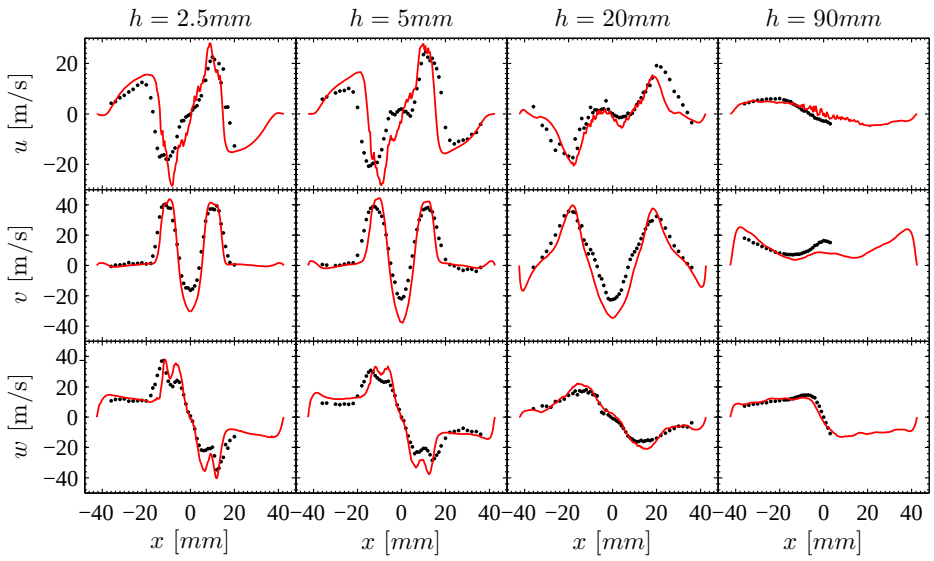

Figure 6. Mean velocity for flame A, comparing experimental measurement (symbols) and LES-results with Vreman model (red line).

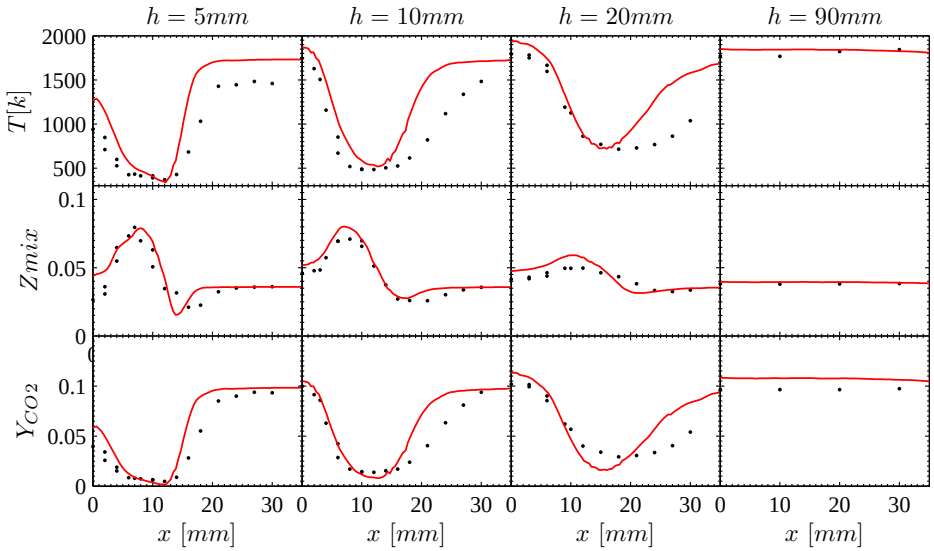

Figure 7. Mean temperature, mixture fraction and $CO2$ mass-fraction for flame A, comparing experimental measurement (symbols) and LES-results with Vreman model (red line).

parison of temperature profiles, presented in the first row, show that the predictions are in overall good agreement, however, the temperature is overpredicted away from the flame-region. This is not unexpected as the utilized FPV-combustion-model does not account for heat lost effects. Similar overpredictions for the near-wall temperature were observed in the study by Moureau et al.,[39] in which they also utilized adiabatic flamelets to model the reaction in a confined burner. Aside from the temperature, mean profiles for $\widetilde{Z}$ and $\widetilde{Y}_{\mathrm{CO}_2}$ at locations $h = 5$ mm and 10 mm are in reasonable agreement with measurements. This suggests that the mixing and reaction is well captured with this combustion model. Apart from the discrepancy in the near-wall region, the mean temperature profiles for $h \leq 20$ mm are slightly overpredicted along the centerline and the temperature profiles

are more confined compared to the experiments. These features are also reflected in the mixture fraction profile, and might be attributed to a shift in the predicted velocity profile. With increasing downstream distance, the flow approaches an equilibrium composition, which is well predicted by the LES.

V. Conclusions

Large-eddy simulations of a model-gas turbine combustor are performed for isothermal and reacting operating conditions. For the simulation of this geometrically-complex combustor configuration an unstructured LES-solver in conjunction with a FPV-flamelet-based combustion model was employed. The computational domain was discretized using a hex-dominated unstructured mesh. Given the complexity of the flow-field, simulation results for both non-reacting and reacting cases are overall in good agreement. It was found that the flow-field structure is particularly sensitive to the subgrid-closure model, and it was concluded form this study that the Vreman model accurately captures the inner and outer recirculation structure that is presented in this combustor. The comparison of profiles for temperature and mixture fraction show that the simulation captures the flame-location and mixing, which is largely confined to the lower part of the combustor. The observed overpredictions of the temperature away from the flame suggests that wall-heat losses require consideration, and this issue will be addressed in future work. In addition, comprehensive mesh-refinement studies will be performed to further assess the accuracy of the simulation and robustness of the subgrid closure models.

References

[1]Menon, S., "Modeling Pollutant Emission and Lean Blow Out in Gas Turbine Combustors," *AIAA Paper 2003-4496*, 2003.

[2]Menon, S., "Acoustic-vortex-flame interactions in gas turbines," *Progress in Astronautics and Aeronautics*, edited by T. C. Lieuwen and V. Yang, 2005, pp. 277–314.

[3]Huang, Y. and Yang, V., "Bifurcation of flame structure in a lean-premixed swirl-stabilized combustor," *Combust. Flame*, Vol. 136, 2004, pp. 383–389.

[4]Huang, Y., Wang, S., and Yang, V., "Flow and flame dynamics of lean premixed swirl injectors," *Progress in Astronautics and Aeronautics*, edited by T. C. Lieuwen and V. Yang, 2005, pp. 213–276.

[5]Pitsch, H. and Duchamp De Lageneste, L., "Large-eddy simulation of premixed turbulent combustion using a level-set approach," *Proc. Combust. Inst.*, Vol. 29, 2003, pp. 2001–2008.

[6]Knudsen, E. and Pitsch, H., "A dynamic model for the turbulent burning velocity for large eddy simulation of premixed combustion," *Combust. Flame*, Vol. 154, No. 4, 2008, 740-760.

[7]Pitsch, H., "A consistent level set formulation for large-eddy simulation of premixed turbulent combustion," *Combust. Flame*, Vol. 143, No. 4, 2005, pp. 587–598.

[8]Klimenko, A. Y. and Bilger, R. W., "Conditional moment closure for turbulent combustion," *Prog. Energy Combust. Sci.*, Vol. 25, No. 6, 1999, pp. 595–687.

[9]Kim, S. H. and Huh, K. Y., "Second-order conditional moment closure modeling of turbulent piloted jet diffusion flames," *Combust. Flame*, Vol. 138, 2004, pp. 336–352.

[10]Kronenburg, A., Bilger, R. W., and Kent, J. H., "Second-order conditional moment closure for turbulent jet diffusion flames," *Proc. Combust. Inst.*, Vol. 27, 1998, pp. 1097–1104.

[11]Triantafyllidis, A., Mastorakos, E., and Eggels, R. L. G. M., "Large Eddy Simulations of forced ignition of a non-premixed bluff-body methane flame with Conditional Moment Closure," *Combust. Flame*, Vol. 156, 2009, pp. 2328–2345.

[12]Roomina, M. R. and Bilger, R. W., "Conditional moment closure (CMC) predictions of a turbulent methane-air jet flame," *Combust. Flame*, Vol. 125, No. 3, 2001, pp. 1176–1195.

[13]Sommerer, Y., Galley, D., Poinsot, T., Ducruix, S., Lacas, F., and Veynante, D., "Large eddy simulation and experimental study of flashback and blow-off in a lean partially premixed swirled burner," *J. Turb.*, Vol. 5, No. 1, 2004, pp. 37.

[14]Angelberger, C., Veynante, D., and Egolfopoulos, F., "LES of chemical and acoustic forcing of a premixed dump combustor," *Flow, Turb. Combust.*, Vol. 65, No. 2, 2000, pp. 205–222.

[15]Martin, C. E., Benoit, L., Sommerer, Y., Nicoud, F., and Poinsot, T., "Large-eddy simulation and acoustic analysis of a swirled staged turbulent combustor," *AIAA J.*, Vol. 44, No. 4, 2006, pp. 741–750.

[16]Colucci, P. J., Jaberi, F. A., Givi, P., and Pope, S. B., "Filtered Density Function for Large Eddy Simulation of Turbulent Reacting Flows," *Phys. Fluids*, Vol. 10, No. 2, 1998, pp. 499–515.

[17]Sheikhi, M. R. H., Drozda, T. G., Givi, P., Jaberi, F. A., and Pope, S. B., "Large eddy simulation of a turbulent nonpremixed piloted methane jet flame (Sandia Flame D)," *Proc. Combust. Inst.*, Vol. 30, 2005, pp. 549–556.

[18]Sheikhi, M. R. H., Givi, P., and Pope, S. B., "Velocity-scalar filtered mass density function for large eddy simulation of turbulent reacting flows," *Phys. Fluids*, Vol. 19, 2007, pp. 095106.

[19]Pierce, C. D. and Moin, P., "Progress-variable approach for large-eddy simulation of non-premixed turbulent combustion," *J. Fluid Mech.*, Vol. 504, 2004, pp. 73–97.

[20]Ihme, M., Cha, C. M., and Pitsch, H., "Prediction of local extinction and re-ignition effects in non-premixed turbulent combustion using a flamelet/progress variable approach," *Proc. Combust. Inst.*, Vol. 30, 2005, pp. 793–800.

[21]Selle, L., Lartigue, G., Poinsot, T., Koch, R., Schildmacher, K.-U. amd Krebs, W., Prade, B., Kaufmann, P., and Veynante, D., "Compressible large eddy simulation of turbulent combustion in complex geometry on unstructured meshes," *Combust. Flame*, Vol. 137, 2004, pp. 489–505.

[22]Wegner, B., Staufer, M., Sadiki, A., and Janicka, J., "Study of flow and mixing in a generic GT combustor using LES," *Flow, Turb. Combust.*, Vol. 79, 2007, pp. 389–403.

[23]Ihme, M. and Pitsch, H., "Modeling of Radiation and NO Formation in Turbulent Non-premixed Flames Using a Flamelet/Progress Variable Formulation," *Phys. Fluids*, Vol. 20, 2008, pp. 055110.

[24]Kim, W.-W. and Syed, S., "Large-Eddy Simulation Needs for Gas Turbine Combustor Design," *AIAA Paper 2004-331*, 2004.

[25]Ham, F., Mattsson, K., and Iaccarino, G., "Accurate and stable finite volume operators for unstructured flow solvers," *Annual Research Briefs, Center for Turbulence Research, NASA Ames/Stanford University*, 2006, pp. 243261.

[26]Ham, F., Mattsson, K., Iaccarino, G., and Moin, P., "Towards Time-Stable and Accurate LES on Unstructured Grids," *Complex Effects in Large Eddy Simulations*, edited by S. C. Kassinos, C. A. Langer, G. Iaccarino, and P. Moin, Vol. 56, Springer Berlin Heidelberg, Berlin, Heidelberg, 2007, pp. 235–249.

[27]Ham, F., "An efficient scheme for large eddy simulation of low-Ma combustion in complex configurations," *Annual Research Briefs (Center for Turbulence Research, Stanford University)*, 2007, pp. 41.

[28]Falgout, R. D. and Yang, U. M., "hypre: a Library of High Performance Preconditioners," *Preconditioners, Lecture Notes in Computer Science*, 2002, p. 632641.

[29]Germano, M., Piomelli, U., Moin, P., and Cabot, W. H., "A dynamic subgrid-scale eddy viscosity model," *Phys. Fluids A*, Vol. 3, No. 7, 1991, pp. 1760–1765.

[30]Lilly, D. K., "A proposed modification of the Germano subgrid-scale closure method," *Phys. Fluids A*, Vol. 4, No. 3, 1992, pp. 633–635.

[31]Vreman, A. W., "An eddy-viscosity subgrid-scale model for turbulent shear flow: Algebraic theory and applications," *Physics of Fluids*, Vol. 16, No. 10, Sept. 2004, pp. 3670–3681.

[32]Pierce, C. D. and Moin, P., "Progress-variable approach for large eddy simulation of turbulent combustion," Report No. TF-80, Stanford University, 2001.

[33]Peters, N., "Local quenching due to flame stretch and non-premixed turbulent combustion," *Combust. Sci. Tech.*, Vol. 30, 1983, pp. 1–17.

[34]Peters, N., "Laminar diffusion flamelet models in non-premixed turbulent combustion," *Prog. Energy Combust. Sci.*, Vol. 10, No. 3, 1984, pp. 319–339.

[35]Weigand, P., Meier, W., Duan, X., Stricker, W., and Aigner, M., "Investigations of swirl flames in a gas turbine model combustor: I. Flow field, structures, temperature, and species distributions," *Combustion and Flame*, Vol. 144, No. 1-2, Jan. 2006, pp. 205–224.

[36]Meier, W., Duan, X., and Weigand, P., "Investigations of swirl flames in a gas turbine model combustor: II. Turbulence-chemistry interactions," *Combustion and Flame*, Vol. 144, No. 1-2, Jan. 2006, pp. 225–236.

[37]Widenhorn, A., Noll, B., and Aigner, M., "Numerical Study of a Non-Reacting Turbulent Flow in a Gas Turbine Model Combustor," *47 th AIAA Aerospace Sciences Meeting Including the New Horizons Forum and Aerospace Exposition*, AIAA, Orlando, 2009.

[38]Ihme, M., Shunn, L., and Zhang, J., "Regularization of reaction progress variable for application to flamelet-based combustion models," *J. Comp. Phys.*, Vol. 231, 2012, pp. 7715–7721.

[39]Moureau, V., Domingo, P., and Vervisch, L., "From Large-Eddy Simulation to Direct Numerical Simulation of a lean premixed swirl flame: Filtered laminar flame-PDF modeling," *Combustion and Flame*, Vol. 158, No. 7, July 2011, pp. 1340–1357.